Supporting Information

Photoinduced electron-transfer strategy for switchable fluorescence and phosphorescence in lanthanide-based coordination polymers

Yu-Juan Ma,†[a] Fei Xu,†[a] Xin-Ye Ren,[a] Fan-Yao Chen,[a] Jie Pan,[a] Jin-Hua Li,*[a] Song-De Han,*[a] and Guo-Ming Wang*[a]

[a] College of Chemistry and Chemical Engineering, Key Laboratory of Shandong Provincial Universities for Functional Molecules and Materials, Qingdao University, Qingdao, Shandong 266071, P. R. China

E-mail: gmwang_pub@163.com; hansongde@qdu.edu.cn; jinhuali1978@163.com

† These authors contributed equally to this work.

Contents

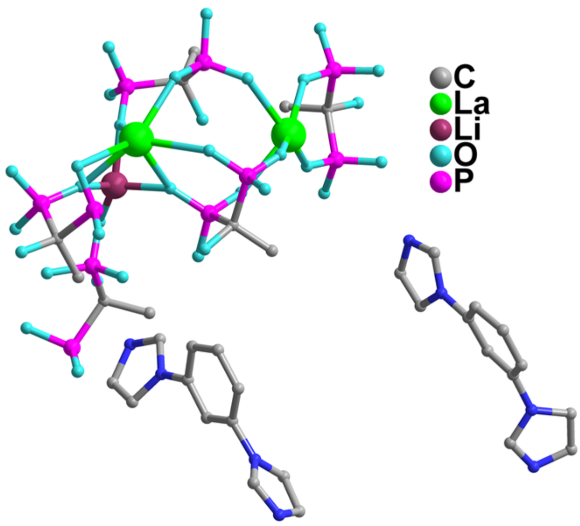

Figure S1. The asymmetric unit of **La**.

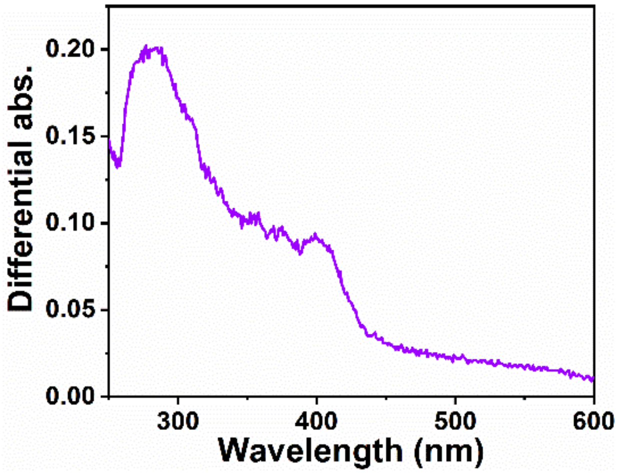

Figure S2. Differential absorption spectra before and after irradiation for 30 min.

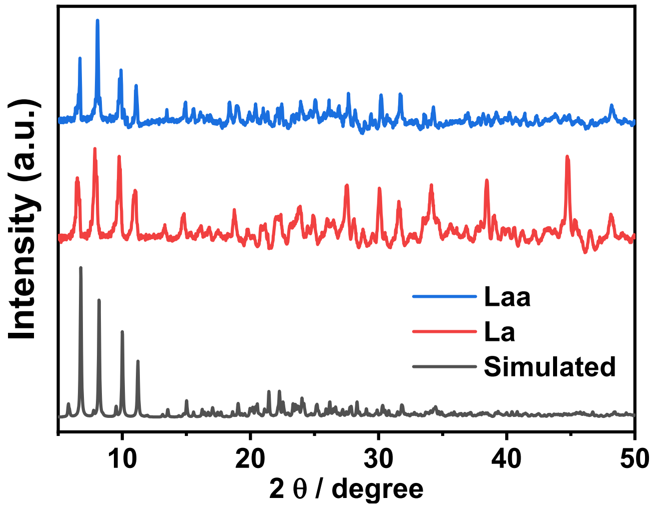

Figure S3. The PXRD spectra of **La** and **Laa**.

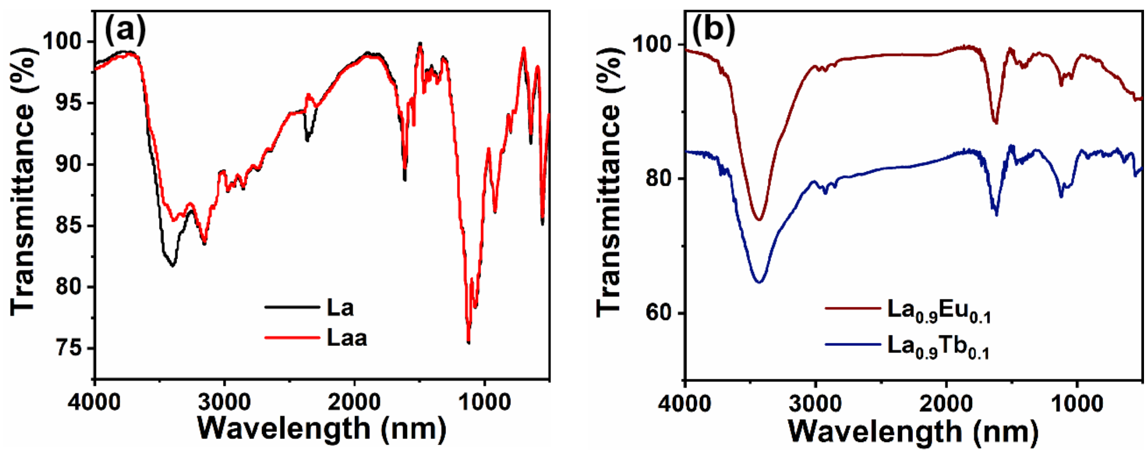

Figure S4. The IR spectra of **La**, **Laa** (a), $\mathbf{La_{0.9}Eu_{0.1}}$ and $\mathbf{La_{0.9}Tb_{0.1}}$ (b).

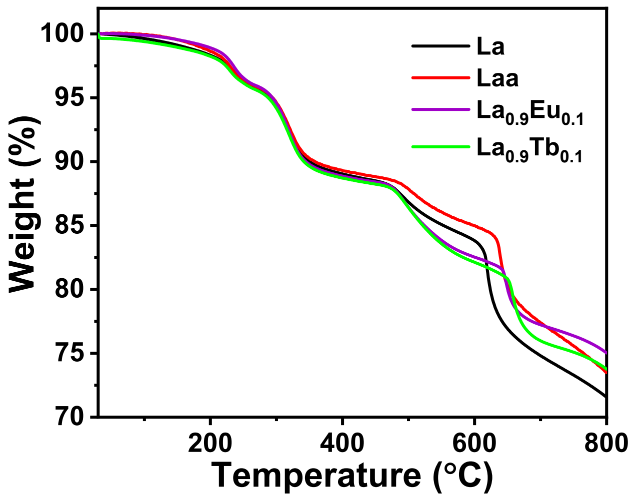

Figure S5. TGA plots of a series of CPs.

	No.	CIE x	CIE y	Peak	Peak Intensity
	1	0.2113	0.1818	335	4621
	2	0.2088	0.1689	335	3678
	3	0.2047	0.1594	336	3160
	4	0.1995	0.1554	409	2893
	5	0.1959	0.1591	415	3270
	6	0.1949	0.1637	415	3381
	7	0.1948	0.1705	420	3466
	8	0.1983	0.1902	424	3279
	9	0.202	0.2049	425	3147

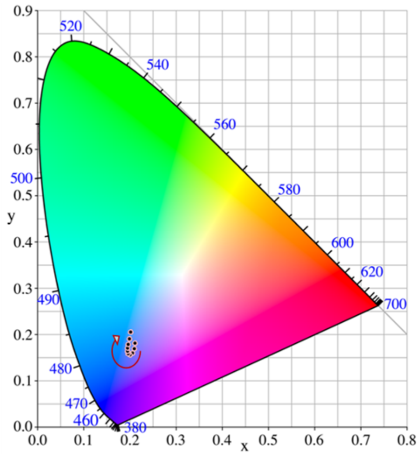

Figure S6. The corresponding CIE chromaticity coordinates of **La** excited by 280 nm UV light.

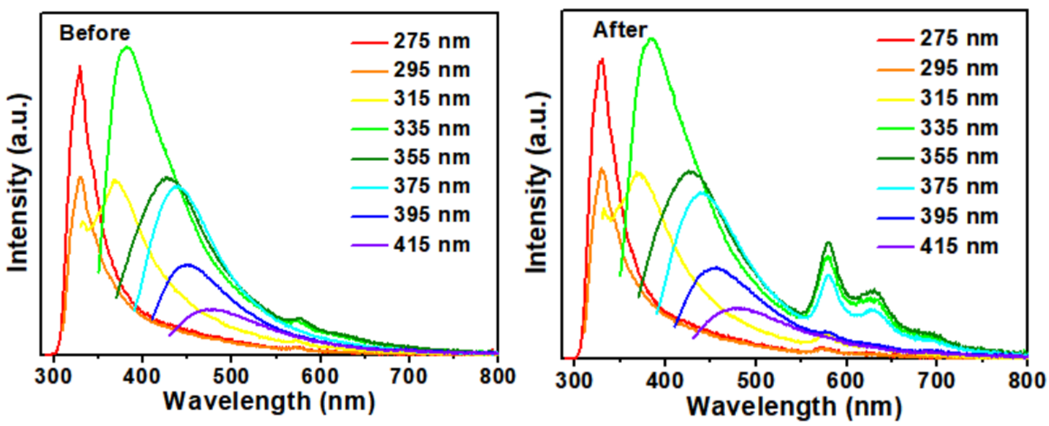

Figure S7. The excitation wavelength-dependent PL spectra of **La** and **Laa.**

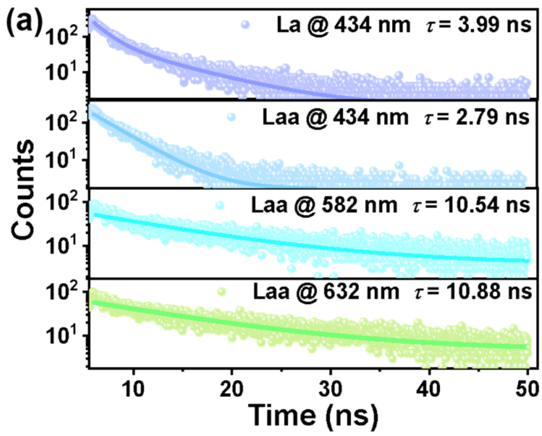

(b)

No.	CIE x	CIE y	Peak	Peak Intensity
1	0.182	0.1543	434	860.8
2	0.1867	0.1625	436	717.9
3	0.197	0.1742	438	600.7
4	0.2124	0.1882	437	519.4
5	0.2345	0.2062	439	454
6	0.2609	0.2264	439	401.9
7	0.2856	0.2455	439	364.4
8	0.3023	0.2604	438	353.2

Figure S8. (a) The decay curves monitored in different emission peaks; (b) The corresponding CIE coordinates for the irradiation time-dependent fluorescent spectra excited by 370 nm UV light.

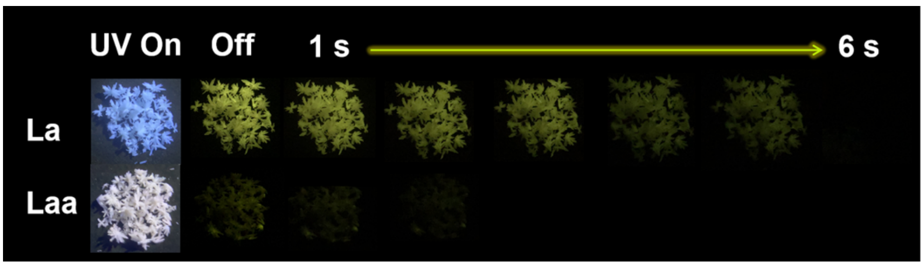

Figure S9. The photographs for **La** and **Laa** taken under a 365 nm UV lamp on and off.

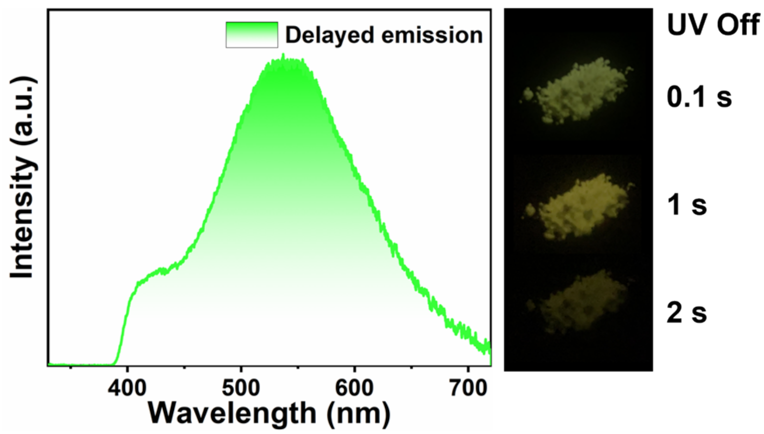

Figure S10. Delayed PL spectra and photographs of TIBP after turning off the 365 nm UV lamp.

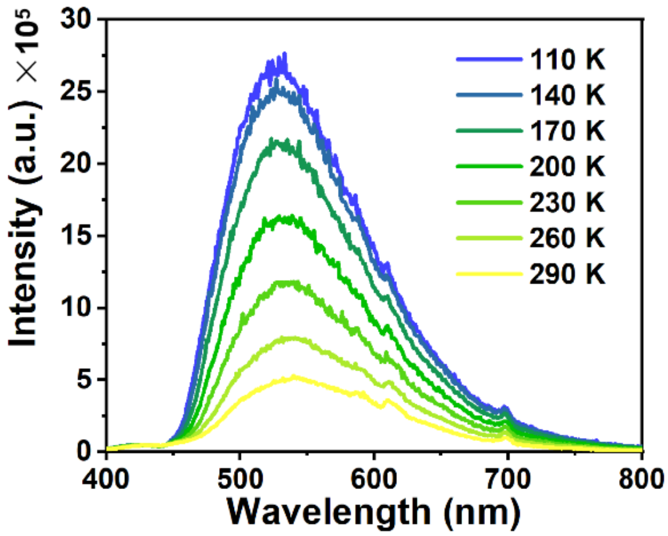

Figure S11. The temperature-dependent delayed emission spectra of **La** excited by 365 nm UV light.

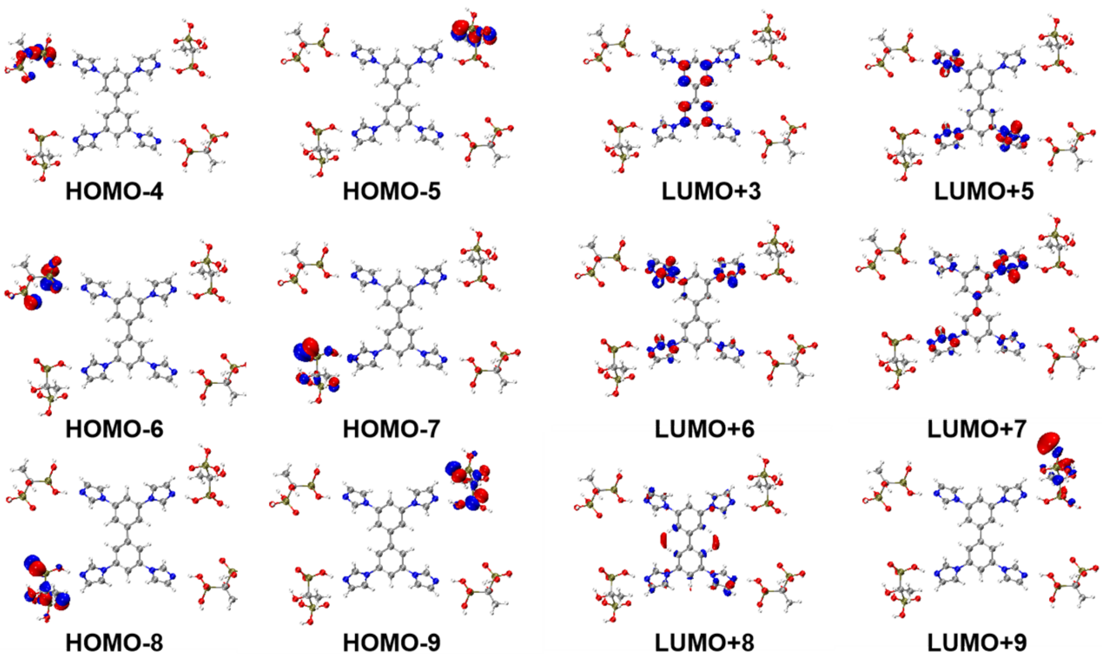

Figure S12. Calculated molecular orbitals.

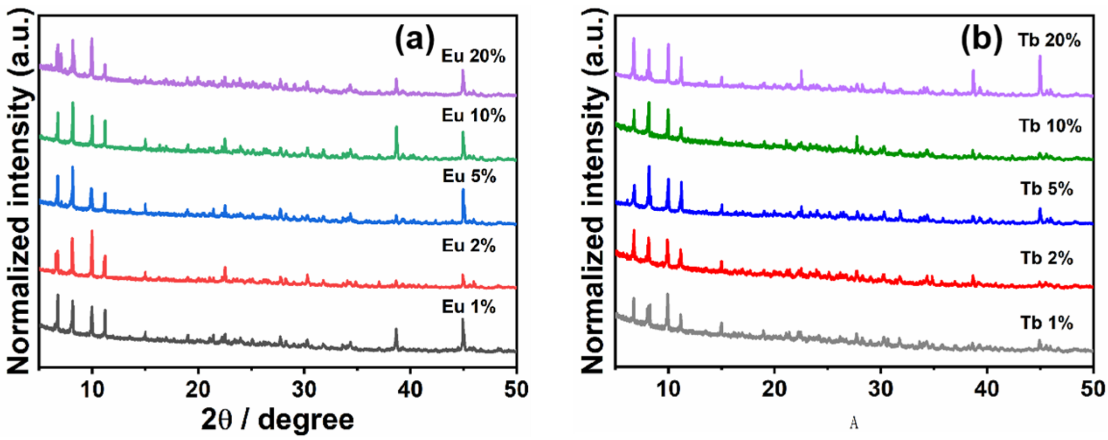

Figure S13. The PXRD spectra of Eu^{3+}/Tb^{3+}-doped CPs.

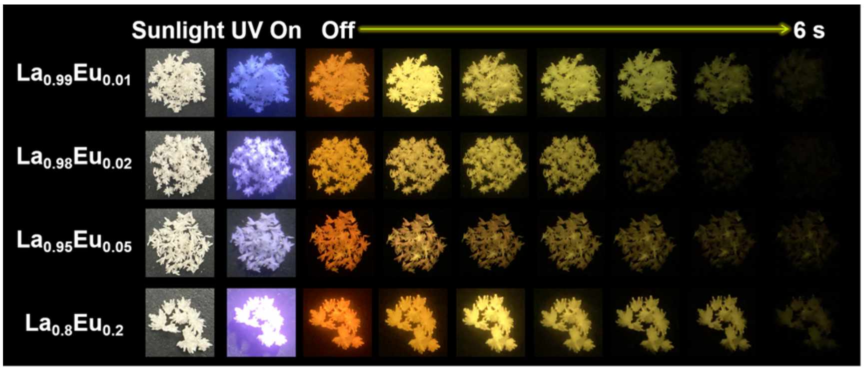

Figure S14. Photographs of different amounts of Eu^{3+}-doped CPs (λ_{ex}=365 nm).

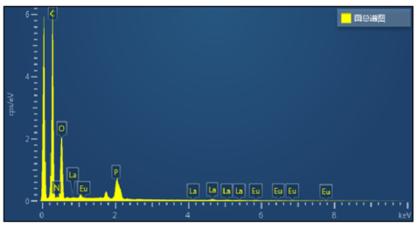

Element	Apparent concentration
C	4.64
N	<0.01
O	3.24
P	0.74
La	0.37
Eu	0.06

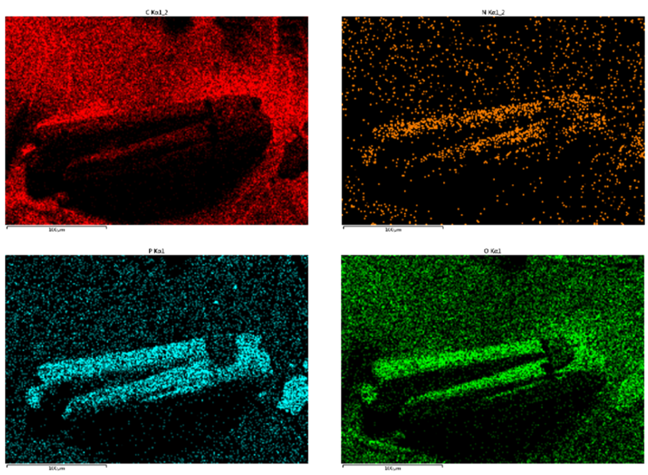

Figure S15. Apparent concentration and elemental mapping images of $\mathbf{La_{0.9}Eu_{0.1}}$.

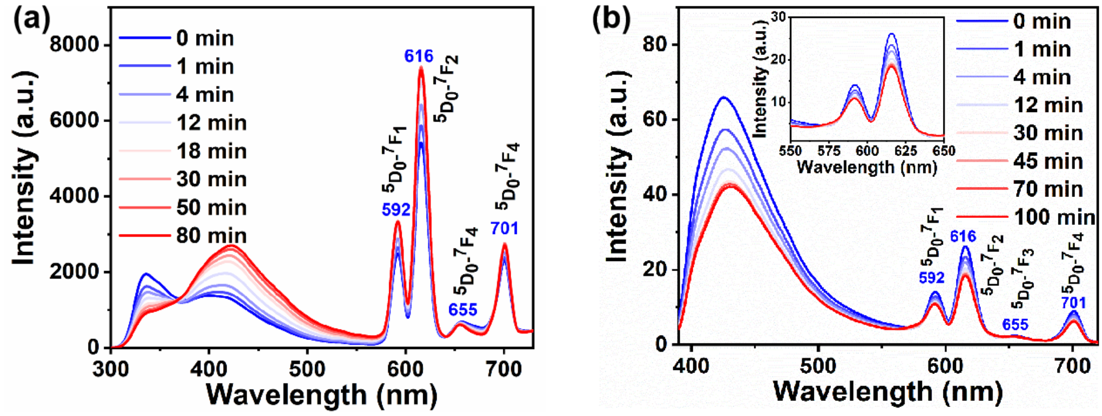

Figure S16. The irradiation time-dependent prompt PL spectra of **$La_{0.9}Eu_{0.1}$** excited by 280 nm (a) and 370 nm UV light (b), respectively.

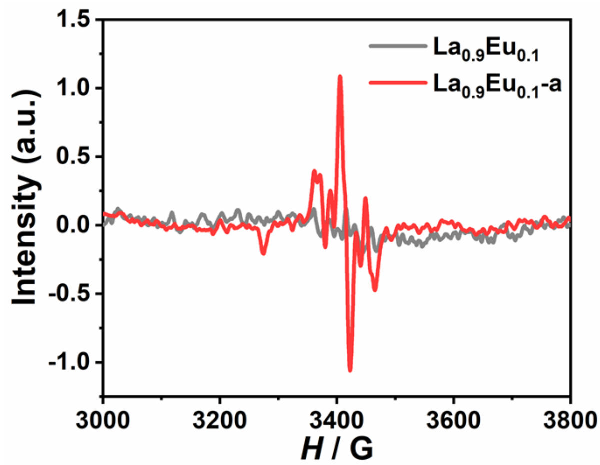

Figure 17. EPR spectra of **$La_{0.9}Eu_{0.1}$** before and after irradiation.

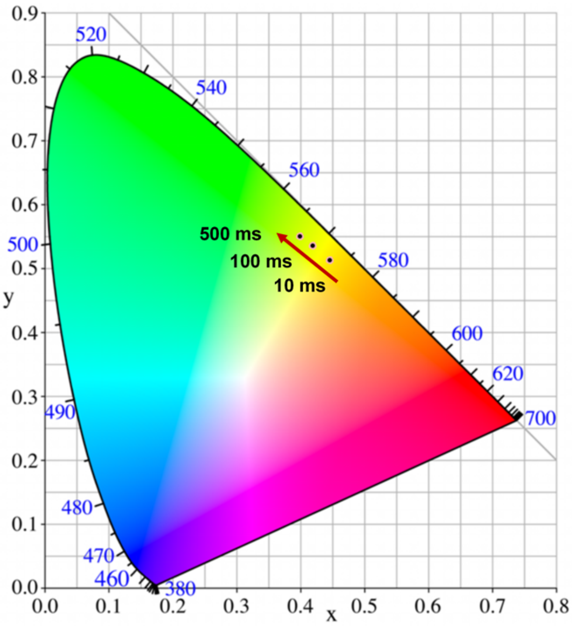

Figure 18. The corresponding CIE chromaticity coordinates of **$La_{0.9}Eu_{0.1}$** at different delay time.

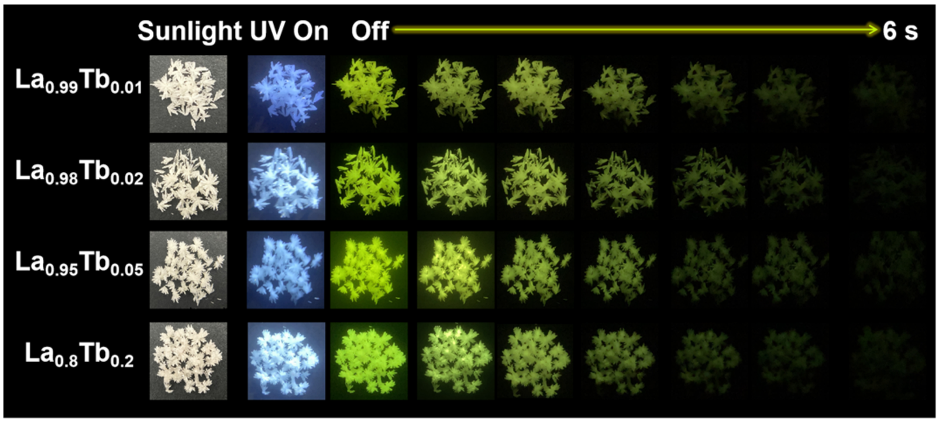

Figure S19. Photographs of different amounts of Tb^{3+}-doped CPs (λ_{ex}=365 nm).

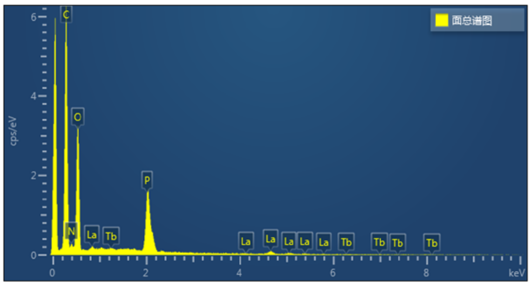

Element	Apparent concentration
C	3.83
N	0.23
O	4.29
P	1.73
La	0.69
Tb	0.11

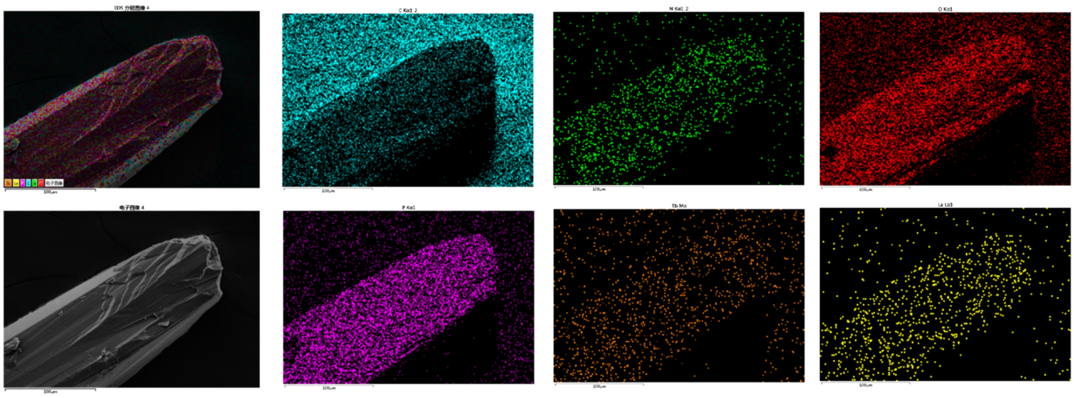

Figure S20. Apparent concentration, SEM and elemental mapping images of $\mathbf{La_{0.9}Tb_{0.1}}$

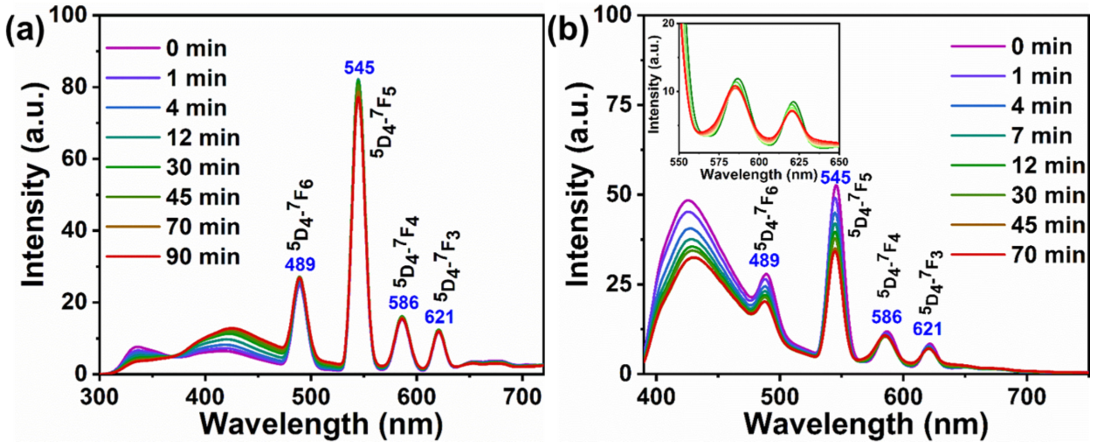

Figure S21. The irradiation time-dependent prompt PL spectra of $\mathbf{La_{0.9}Tb_{0.1}}$ excited by 280 nm (a) and 370 nm UV light (b), respectively.

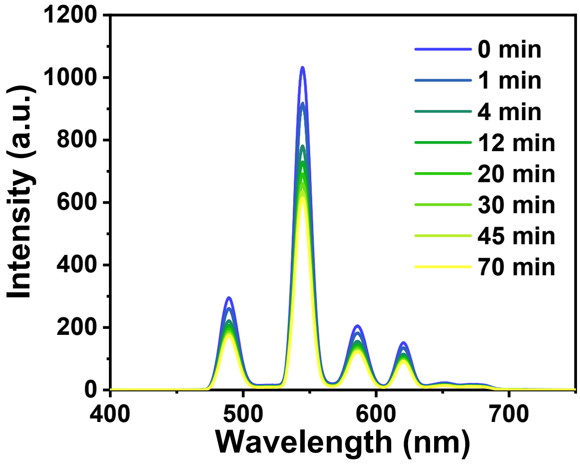

Figure S22. The irradiation time-dependent delayed PL spectra of $\mathbf{La_{0.9}Tb_{0.1}}$ excited by 365 nm UV light.

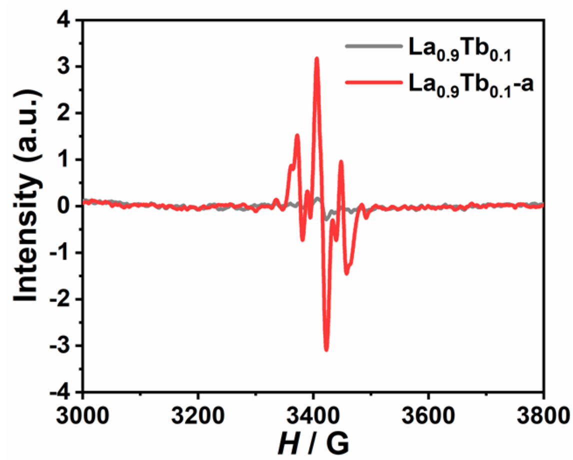

Figure S23. EPR spectra of $\mathbf{La_{0.9}Tb_{0.1}}$ before and after irradiation.

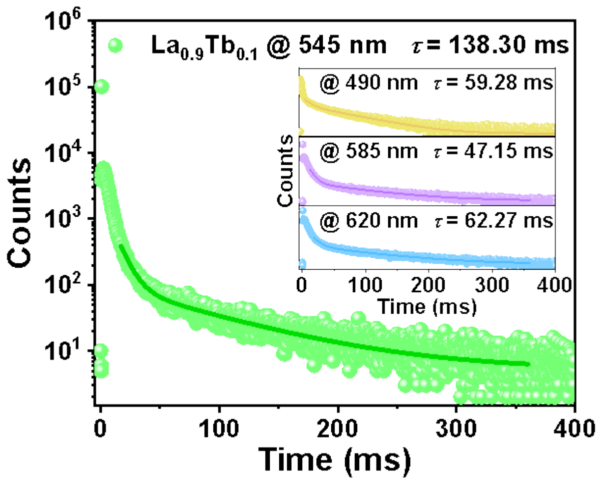

Figure S24. Long-lived decay curves for $\mathbf{La_{0.9}Tb_{0.1}}$.

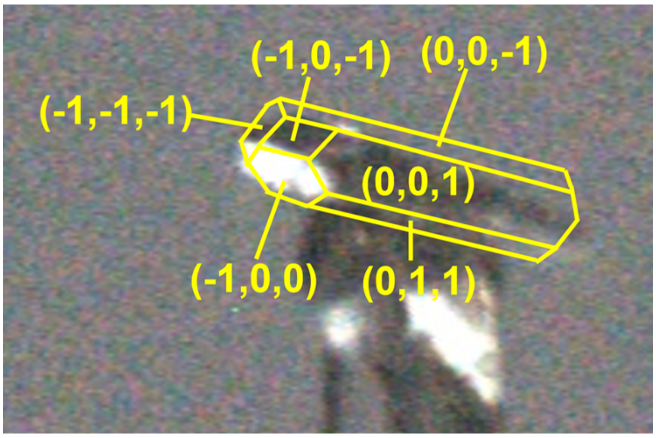

Figure S25. Face index of **La** crystal.

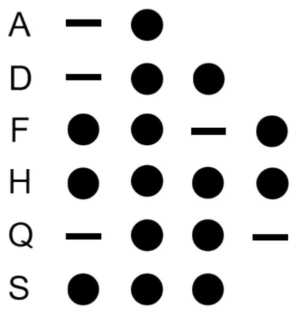

Figure S26. The letters used in Morse code application.

Table S1. Crystal data for **La** and **Laa** at 293 K.

	La	**Laa**
Formula	$C_{34}H_{57}N_8O_{38}P_{10}La_2Li$	$C_{34}H_{57}N_8O_{38}P_{10}La_2Li$
F_w (g mol^{-1})	1780.28	1780.28
λ/Å	0.71073	0.71073
Crystal system	Triclinic	Triclinic
Space group	$P\bar{1}$	$P\bar{1}$
a/Å	12.2018(2)	12.1985(2)
b/Å	16.4476(2)	16.4328(3)
c/Å	16.9585(3)	16.9643(4)
α (°)	68.4420(10)	68.463(2)
β/°	69.632(2)	69.625(2)
γ (°)	79.1400(10)	79.152(2)
V/Å^3	2960.26(9)	2958.14(12)
Z	2	2
D_c/g cm^{-3}	1.991	1.992
μ/mm^{-1}	1.805	1.806
F (000)	1764	1764
Total/unique reflns	42386/10440	44686/10438
R_{int}	0.0547	0.0453
Final R indices	R_1 = 0.0297	R_1 = 0.0334
[I>2σ(I)]	wR_2 = 0.0757	wR_2 = 0.0838
wR_2 (all data)	R_1 = 0.0356 wR_2 = 0.0785	R_1 = 0.0387 wR_2 = 0.0859
GOF on F^2	1.053	1.118

Table S2. SHAPE analysis of the metal ions in **La**.

Metal	Label	Shape	Symmetry	Distortion
La1	OP-8	Octagon	D_{8h}	28.099
La1	HPY-8	Heptagonal pyramid	C_{7v}	23.356
La1	HBPY-8	Hexagonal bipyramid	D_{6h}	16.063
La1	CU-8	Cube	O_h	11.376
La1	SAPR-8	Square antiprism	D_{4d}	1.822
La1	TDD-8	Triangular dodecahedron	D_{2d}	1.543
La1	JGBF-8	Johnson gyrobifastigium J26	D_{2d}	12.413
La1	JETBPY-8	Johnson elongated triangular bipyramid J14	D_{3h}	25.674
La1	JBTPR-8	Biaugmented trigonal prism J50	C_{2v}	2.088
La1	BTPR-8	Biaugmented trigonal prism	C_{2v}	1.325

La1	JSD-8	Snub diphenoid J84	D_{2d}	3.299
La1	TT-8	Triakis tetrahedron	T_d	11.967
La1	ETBPY-8	Elongated trigonal bipyramid	D_{3h}	21.464
La2	HP-7	Heptagon	D_{7h}	30.307
La2	HPY-7	Hexagonal pyramid	C_{6v}	19.300
La2	PBPY-7	Pentagonal bipyramid	D_{5h}	6.446
La2	COC-7	Capped octahedron	C_{3v}	1.963
La2	CTPR-7	Capped trigonal prism	C_{2v}	0.776
La2	JPBPY-7	Johnson pentagonal bipyramid J13	D_{5h}	9.828
La2	JETPY-7	Johnson elongated triangular pyramid J7	C_{3v}	17.900
Li1	TP-3	Trigonal	D_{3h}	3.708
Li1	vT-3	Vacant tetrahedron	C_{3v}	2.570
Li1	fvOC-3	fac-Trivacant octahedron	C_{3v}	6.844

Table S3. Selected bond lengths (Å) and angles (°) for **La** at 293 K.

La(1)-O(1)	2.556(2)	O(1)-P(1)	1.507(2)
La(1)-O(14)	2.533(2)	O(10)-P(3)	1.511(2)
La(1)-O(15)	2.479(2)	O(12)-P(4)	1.509(2)
La(1)-O(20)	2.625(3)	O(13)-P(4)	1.580(3)
La(1)-O(3)#1	2.414(2)	O(14)-P(4)	1.504(2)
La(1)-O(5)#1	2.561(2)	O(15)-P(6)	1.518(2)
La(1)-O(7)	2.563(2)	O(16)-P(6)	1.569(2)
La(1)-O(8)	2.534(2)	O(17)-P(6)	1.498(2)
La(2)-O(10)	2.425(2)	O(19)-P(5)	1.565(3)
La(2)-O(12)	2.561(3)	O(2)-P(1)	1.556(3)
La(2)-O(17)	2.445(2)	O(20)-P(5)	1.511(2)
La(2)-O(22)	2.475(2)	O(21)-P(5)	1.501(3)
La(2)-O(24)#2	2.481(2)	O(22)-P(7)	1.509(3)
La(2)-O(26)#2	2.569(2)	O(23)-P(7)	1.566(3)
La(2)-O(28)	2.476(3)	O(24)-P(7)	1.497(3)
O(24)-La(2)#2	2.481(2)	O(26)-P(8)	1.510(3)
Li(1)-O(20)	1.964(7)	O(27)-P(8)	1.575(3)
Li(1)-O(30)	1.918(7)	O(28)-P(8)	1.490(3)
Li(1)-O(7)	1.959(7)	O(3)-P(1)	1.505(2)
Li(1)-O(8)	2.082(7)	O(30)-P(9)	1.532(3)
O(26)-La(2)#2	2.569(2)	O(31)-P(9)	1.521(3)

O(3)-La(1)#1	2.414(2)	O(32)-P(9)	1.526(3)
O(5)-La(1)#1	2.561(2)	O(34)-P(10)	1.493(3)
C(3)-P(3)	1.826(4)	O(35)-P(10)	1.601(3)
C(3)-P(4)	1.844(4)	O(36)-P(10)	1.500(3)
C(5)-P(5)	1.843(4)	O(5)-P(2)	1.526(2)
C(5)-P(6)	1.853(4)	O(6)-P(2)	1.557(2)
C(7)-P(7)	1.845(4)	O(7)-P(2)	1.507(2)
C(7)-P(8)	1.832(4)	O(8)-P(3)	1.513(2)
C(9)-P(10)	1.849(3)	O(9)-P(3)	1.559(3)
C(9)-P(9)	1.850(4)		

O(1)-La(1)-O(20)	130.23(8)	O(24)#2-La(2)-O(12)	72.25(8)
O(1)-La(1)-O(5)#1	93.96(8)	O(24)#2-La(2)-O(26)#2	74.35(8)
O(1)-La(1)-O(7)	72.02(8)	O(24)-P(7)-C(7)	106.57(15)
O(1)-P(1)-C(1)	109.71(15)	O(24)-P(7)-O(22)	115.54(16)
O(1)-P(1)-O(2)	110.08(14)	O(24)-P(7)-O(23)	112.78(14)
O(10)-La(2)-O(12)	75.97(8)	O(26)-P(8)-C(7)	106.70(15)
O(10)-La(2)-O(17)	102.23(8)	O(26)-P(8)-O(27)	110.22(15)
O(10)-La(2)-O(22)	132.39(9)	O(27)-P(8)-C(7)	108.48(16)
O(10)-La(2)-O(24)#2	90.36(8)	O(28)-La(2)-O(12)	140.45(8)
O(10)-La(2)-O(26)#2	150.92(9)	O(28)-La(2)-O(24)#2	77.02(9)
O(10)-La(2)-O(28)	79.99(8)	O(28)-La(2)-O(26)#2	118.90(8)
O(10)-P(3)-C(3)	107.60(15)	O(28)-P(8)-C(7)	109.59(15)
O(10)-P(3)-O(8)	114.16(15)	O(28)-P(8)-O(26)	116.45(16)
O(10)-P(3)-O(9)	109.03(15)	O(28)-P(8)-O(27)	105.21(14)
O(12)-La(2)-O(26)#2	75.84(8)	O(3)#1-La(1)-O(1)	116.58(8)
O(12)-P(4)-C(3)	109.37(15)	O(3)#1-La(1)-O(14)	146.93(8)
O(12)-P(4)-O(13)	110.95(14)	O(3)#1-La(1)-O(15)	89.14(8)
O(13)-P(4)-C(3)	106.24(16)	O(3)#1-La(1)-O(20)	76.80(8)
O(14)-La(1)-O(1)	72.70(7)	O(3)#1-La(1)-O(5)#1	71.60(8)
O(14)-La(1)-O(20)	123.24(8)	O(3)#1-La(1)-O(7)	75.46(7)
O(14)-La(1)-O(5)#1	76.25(7)	O(3)#1-La(1)-O(8)	136.62(8)
O(14)-La(1)-O(7)	134.98(7)	O(3)-P(1)-C(1)	107.01(14)
O(14)-La(1)-O(8)	74.93(8)	O(3)-P(1)-O(1)	110.13(14)
O(14)-P(4)-C(3)	109.51(14)	O(3)-P(1)-O(2)	112.18(15)

O(14)-P(4)-O(12)	115.06(14)	O(30)-Li(1)-O(20)	133.4(4)
O(14)-P(4)-O(13)	105.30(14)	O(30)-Li(1)-O(7)	118.4(3)
O(15)-La(1)-O(1)	148.32(8)	O(30)-Li(1)-O(8)	122.9(3)
O(15)-La(1)-O(14)	75.71(8)	O(30)-P(9)-C(9)	108.60(16)
O(15)-La(1)-O(20)	70.93(8)	O(31)-P(9)-C(9)	106.03(16)
O(15)-La(1)-O(5)#1	76.12(8)	O(31)-P(9)-O(30)	109.99(14)
O(15)-La(1)-O(7)	135.99(8)	O(31)-P(9)-O(32)	112.98(16)
O(15)-La(1)-O(8)	95.49(8)	O(32)-P(9)-C(9)	107.33(15)
O(15)-P(6)-C(5)	108.84(15)	O(32)-P(9)-O(30)	111.63(15)
O(15)-P(6)-O(16)	110.74(14)	O(34)-P(10)-C(9)	111.17(17)
O(16)-P(6)-C(5)	109.04(16)	O(34)-P(10)-O(35)	109.52(18)
O(17)-La(2)-O(12)	76.81(8)	O(34)-P(10)-O(36)	116.15(17)
O(17)-La(2)-O(22)	79.21(8)	O(35)-P(10)-C(9)	101.42(16)
O(17)-La(2)-O(24)#2	142.53(9)	O(36)-P(10)-C(9)	109.70(16)
O(17)-La(2)-O(26)#2	78.06(8)	O(36)-P(10)-O(35)	107.81(17)
O(17)-La(2)-O(28)	139.55(9)	O(5)#1-La(1)-O(20)	134.11(7)
O(17)-P(6)-C(5)	106.75(16)	O(5)#1-La(1)-O(7)	133.03(7)
O(17)-P(6)-O(15)	114.72(15)	O(5)-P(2)-C(1)	107.47(15)
O(17)-P(6)-O(16)	106.57(14)	O(5)-P(2)-O(6)	106.21(13)
O(19)-P(5)-C(5)	106.36(16)	O(6)-P(2)-C(1)	108.04(15)
O(2)-P(1)-C(1)	107.62(15)	O(7)-La(1)-O(20)	65.52(7)
O(20)-Li(1)-O(8)	85.6(3)	O(7)-Li(1)-O(20)	91.4(3)
O(20)-P(5)-C(5)	105.61(15)	O(7)-Li(1)-O(8)	94.9(3)
O(20)-P(5)-O(19)	108.72(15)	O(7)-P(2)-C(1)	107.15(14)
O(21)-P(5)-C(5)	107.75(15)	O(7)-P(2)-O(5)	115.46(13)
O(21)-P(5)-O(19)	110.03(15)	O(7)-P(2)-O(6)	112.22(14)
O(21)-P(5)-O(20)	117.73(15)	O(8)-La(1)-O(1)	78.70(8)
O(22)-La(2)-O(12)	146.50(8)	O(8)-La(1)-O(20)	64.37(8)
O(22)-La(2)-O(24)#2	117.48(8)	O(8)-La(1)-O(5)#1	151.15(7)
O(22)-La(2)-O(26)#2	76.57(9)	O(8)-La(1)-O(7)	71.49(7)
O(22)-La(2)-O(28)	70.89(8)	O(8)-P(3)-C(3)	109.21(16)
O(22)-P(7)-C(7)	107.66(15)	O(8)-P(3)-O(9)	110.20(14)
O(22)-P(7)-O(23)	107.21(15)	O(9)-P(3)-C(3)	106.32(16)
O(23)-P(7)-C(7)	106.63(16)		

Symmetry code: #1: -x+2, -y+1, -z; #2: -x+1, -y, -z+1; #3: -x+1, -y+2, -z; #4: -x, -y+1, -z+1.

Table S4. Selected bond lengths (Å) and angles (°) for **Laa** at 293 K.

La(1)-O(1)	2.560(3)	O(10)-P(4)	1.503(3)
La(1)-O(13)	2.524(3)	O(12)-P(3)	1.576(3)
La(1)-O(15)	2.623(3)	O(13)-P(3)	1.511(3)
La(1)-O(19)	2.477(3)	O(14)-P(3)	1.507(3)
La(1)-O(3)#3	2.412(3)	O(15)-P(6)	1.510(3)
La(1)-O(6)#3	2.560(3)	O(16)-P(6)	1.562(3)
La(1)-O(7)	2.562(3)	O(17)-P(6)	1.504(3)
La(1)-O(8)	2.534(3)	O(19)-P(5)	1.512(3)
La(2)-O(10)	2.427(3)	O(2)-P(1)	1.553(3)
La(2)-O(14)	2.559(3)	O(20)-P(5)	1.563(3)
La(2)-O(21)	2.440(3)	O(21)-P(5)	1.504(3)
La(2)-O(22)	2.473(3)	O(22)-P(7)	1.492(3)
La(2)-O(24)#4	2.560(3)	O(23)-P(7)	1.572(3)
La(2)-O(26)#4	2.476(3)	O(24)-P(7)	1.510(3)
La(2)-O(28)	2.473(3)	O(26)-P(8)	1.498(3)
Li(1)-O(15)	1.960(8)	O(27)-P(8)	1.565(3)
Li(1)-O(34)	1.914(8)	O(28)-P(8)	1.510(3)
Li(1)-O(7)	1.957(8)	O(29)-P(10)	1.600(4)
Li(1)-O(8)	2.085(8)	O(3)-P(1)	1.511(3)
C(1)-P(1)	1.835(4)	O(30)-P(10)	1.493(3)
C(1)-P(2)	1.843(4)	O(31)-P(10)	1.501(3)
C(3)-P(3)	1.841(4)	O(33)-P(9)	1.528(3)
C(3)-P(4)	1.832(4)	O(34)-P(9)	1.527(3)
C(5)-P(5)	1.859(4)	O(35)-P(9)	1.522(3)
C(5)-P(6)	1.841(4)	O(5)-P(2)	1.555(3)
C(7)-P(7)	1.834(4)	O(6)-P(2)	1.525(3)
C(7)-P(8)	1.844(4)	O(7)-P(2)	1.505(3)
C(9)-P(10)	1.845(5)	O(8)-P(4)	1.514(3)
C(9)-P(9)	1.853(4)	O(9)-P(4)	1.560(3)
O(1)-P(1)	1.510(3)		
O(1)-La(1)-O(15)	130.14(9)	O(23)-P(7)-C(7)	108.56(19)
O(1)-La(1)-O(6)#3	94.06(9)	O(24)-P(7)-C(7)	106.74(18)
O(1)-La(1)-O(7)	72.10(9)	O(24)-P(7)-O(23)	110.73(19)

O(1)-P(1)-C(1)	109.70(18)	O(26)#4-La(2)-O(14)	72.35(10)
O(1)-P(1)-O(3)	110.10(17)	O(26)#4-La(2)-O(24)#4	74.30(9)
O(10)-La(2)-O(14)	75.86(9)	O(26)-P(8)-C(7)	106.56(18)
O(10)-La(2)-O(21)	102.13(10)	O(26)-P(8)-O(27)	112.87(18)
O(10)-La(2)-O(22)	80.03(10)	O(26)-P(8)-O(28)	115.78(19)
O(10)-La(2)-O(24)#4	151.16(10)	O(27)-P(8)-C(7)	106.46(18)
O(10)-La(2)-O(26)#4	90.55(10)	O(28)-La(2)-O(14)	146.57(10)
O(10)-La(2)-O(28)	132.24(10)	O(28)-La(2)-O(22)	70.96(9)
O(10)-P(4)-C(3)	107.85(18)	O(28)-La(2)-O(24)#4	76.47(10)
O(10)-P(4)-O(8)	114.42(18)	O(28)-La(2)-O(26)#4	117.58(10)
O(10)-P(4)-O(9)	109.18(18)	O(28)-P(8)-C(7)	107.48(18)
O(12)-P(3)-C(3)	105.93(18)	O(28)-P(8)-O(27)	107.20(17)
O(13)-La(1)-O(1)	72.56(9)	O(29)-P(10)-C(9)	101.3(2)
O(13)-La(1)-O(15)	123.24(9)	O(3)#3-La(1)-O(1)	116.57(10)
O(13)-La(1)-O(6)#3	76.25(9)	O(3)#3-La(1)-O(13)	147.06(9)
O(13)-La(1)-O(7)	134.96(9)	O(3)#3-La(1)-O(15)	76.89(10)
O(13)-La(1)-O(8)	75.01(9)	O(3)#3-La(1)-O(19)	89.35(10)
O(13)-P(3)-C(3)	109.32(18)	O(3)#3-La(1)-O(6)#3	71.67(9)
O(13)-P(3)-O(12)	105.58(16)	O(3)#3-La(1)-O(7)	75.30(9)
O(14)-La(2)-O(24)#4	76.19(10)	O(3)#3-La(1)-O(8)	136.51(10)
O(14)-P(3)-C(3)	109.74(18)	O(3)-P(1)-C(1)	107.15(17)
O(14)-P(3)-O(12)	110.78(16)	O(3)-P(1)-O(2)	112.20(17)
O(14)-P(3)-O(13)	115.05(17)	O(30)-P(10)-C(9)	111.3(2)
O(15)-Li(1)-O(8)	85.5(3)	O(30)-P(10)-O(29)	109.8(2)
O(15)-P(6)-C(5)	105.47(18)	O(30)-P(10)-O(31)	116.1(2)
O(15)-P(6)-O(16)	108.74(18)	O(31)-P(10)-C(9)	109.6(2)
O(16)-P(6)-C(5)	106.17(19)	O(31)-P(10)-O(29)	107.5(2)
O(17)-P(6)-C(5)	107.83(19)	O(33)-P(9)-C(9)	107.32(19)
O(17)-P(6)-O(15)	117.62(17)	O(34)-Li(1)-O(15)	133.8(4)
O(17)-P(6)-O(16)	110.33(18)	O(34)-Li(1)-O(7)	118.5(4)
O(19)-La(1)-O(1)	148.23(9)	O(34)-Li(1)-O(8)	122.5(4)
O(19)-La(1)-O(13)	75.76(9)	O(34)-P(9)-C(9)	108.71(18)
O(19)-La(1)-O(15)	70.89(9)	O(34)-P(9)-O(33)	111.67(19)
O(19)-La(1)-O(6)#3	76.16(9)	O(35)-P(9)-C(9)	106.0(2)
O(19)-La(1)-O(7)	135.91(9)	O(35)-P(9)-O(33)	113.05(19)

O(19)-La(1)-O(8)	95.56(10)	O(35)-P(9)-O(34)	109.82(18)
O(19)-P(5)-C(5)	108.69(18)	O(5)-P(2)-C(1)	108.14(18)
O(19)-P(5)-O(20)	110.86(17)	O(6)#3-La(1)-O(15)	134.14(9)
O(2)-P(1)-C(1)	107.81(18)	O(6)#3-La(1)-O(7)	133.07(9)
O(20)-P(5)-C(5)	108.72(19)	O(6)-P(2)-C(1)	107.40(17)
O(21)-La(2)-O(14)	76.85(10)	O(6)-P(2)-O(5)	106.22(16)
O(21)-La(2)-O(22)	139.49(10)	O(7)-La(1)-O(15)	65.47(9)
O(21)-La(2)-O(24)#4	78.16(10)	O(7)-Li(1)-O(15)	91.4(3)
O(21)-La(2)-O(26)#4	142.57(10)	O(7)-Li(1)-O(8)	94.6(3)
O(21)-La(2)-O(28)	79.03(10)	O(7)-P(2)-C(1)	106.97(17)
O(21)-P(5)-C(5)	106.54(19)	O(7)-P(2)-O(5)	112.24(16)
O(21)-P(5)-O(19)	114.98(17)	O(7)-P(2)-O(6)	115.58(16)
O(21)-P(5)-O(20)	106.83(18)	O(8)-La(1)-O(1)	78.49(9)
O(22)-La(2)-O(14)	140.42(9)	O(8)-La(1)-O(15)	64.32(9)
O(22)-La(2)-O(24)#4	118.72(10)	O(8)-La(1)-O(6)#3	151.24(9)
O(22)-La(2)-O(26)#4	77.03(10)	O(8)-La(1)-O(7)	71.35(9)
O(22)-P(7)-C(7)	109.31(18)	O(8)-P(4)-C(3)	109.03(18)
O(22)-P(7)-O(23)	105.22(17)	O(8)-P(4)-O(9)	109.85(17)
O(22)-P(7)-O(24)	116.12(18)	O(9)-P(4)-C(3)	106.17(19)

Symmetry code: #1: -x, -y+1, -z+1; #2: -x+1, -y+2, -z; #3: -x, -y+1, -z+2; #4: -x+1, -y+2, -z+1.

Table S5. The fitting parameters for fluorescence lifetimes.

Compound	λ_{ex} (nm)	λ_{em} (nm)	τ_1 (ns)	A_1 (%)	τ_2 (ns)	A_2 (%)	<τ> (ns)	χ^2
La	295	334	0.6736	50.78	2.301	49.22	1.47	1.0628
	375	434	1.519	42.72	5.835	57.28	3.99	1.0933
Laa	295	334	0.52	60.21	1.624	39.79	0.96	1.0851
		422	3.707	100	---	---	3.707	1.0908
	375	434	2.794	100	---	---	2.794	1.2363
		582	10.54	100	---	---	10.54	1.3097
		632	10.88	100	---	---	10.88	1.2100

Table S6. The fitting parameters for phosphorescence lifetimes.

Compound	λ_{ex} (nm)	λ_{em} (nm)	τ_1 (ms)	A_1 (%)	τ_2 (ms)	A_2 (%)	<τ> (ms)	χ^2
La	365	545	45.10	18.23	298.5	81.77	252.31	1.377
$\mathbf{La_{0.9}Eu_{0.1}}$	365	545	67.90	12.70	329.7	87.30	296.45	1.309
		592	9.705	45.63	69.05	54.37	41.97	1.288
		616	14.75	31.48	80.87	68.52	60.06	1.304
		700	12.59	35.63	71.39	64.37	50.44	1.291
$\mathbf{La_{0.9}Tb_{0.1}}$	365	490	8.635	29.04	81.01	70.96	59.28	1.300
		545	42.17	38.15	197.6	61.85	138.30	1.257
		585	6.501	39.35	73.52	60.65	47.15	1.297
		620	8.675	24.81	79.95	75.19	62.27	1.300

Table S7. Chemical compositions of oxide products investigated by XRF technique.

Compound	La_2O_3	Eu_2O_3	Tb_4O_7	Content (%)
$La_{0.9}Eu_{0.1}$	16.237	1.644	---	8.57
$La_{0.9}Tb_{0.1}$	13.109	---	3.668	19.61

Table S8. Surface area percentage of important facets for **La** by BFDH method

hkl	Multiplicity	dhkl	Distance	Total facet area	% Total facet area
{0 1 0}	2	15.26012853	6.55302476	290.0209611	27.26522235
{0 0 1}	2	15.01937939	6.65806472	263.8286319	24.80284972
{0 1 1}	2	13.05639103	7.65908433	142.7032668	13.41570721
{1 0 0}	2	11.41130963	8.76323606	171.9284164	16.16319898
{1 0 1}	2	10.81457506	9.24678034	96.14342937	9.03856042
{1 1 1}	2	10.43352688	9.58448674	86.88873337	8.16851522
{1 1 0}	2	9.45907731	10.57185566	12.18946177	1.14594609